Dzyaloshinsky-Moriya Anisotropy in the Spin-1/2 Kagome Compound ZnCu3 OH 6 Cl2

Dzyaloshinsky-Moriya Anisotropy in the Spin-1/2 Kagome Compound $ZnCu_3(OH)_6Cl_2$

A. Zorko,[1,2] S. Nellutla,[3] J. van Tol,[3] L. C. Brunel,[3] F. Bert,[1] F. Duc,[4] J.-C. Trombe,[4] M. A. de Vries,[5] A. Harrison,[5] and P. Mendels[1]

[1]*Laboratoire de Physique des Solides, UMR CNRS 8502, Université Paris-Sud 11, 91405 Orsay, France*
[2]*Jožef Stefan Institute, Jamova 39, 1000 Ljubljana, Slovenia*
[3]*National High Magnetic Field Laboratory, FSU, Tallahassee, Florida, USA*
[4]*Centre d'Élaboration des Matériaux et d'Études Structurales, CNRS UPR 8011, 31055 Toulouse, France*
[5]*School of Chemistry and SCEC, The University of Edinburgh, Edinburgh, EH9 3JZ, United Kingdom*

(Received 18 April 2008; published 11 July 2008)

We report the determination of the Dzyaloshinsky-Moriya interaction, the dominant magnetic anisotropy term in the kagome spin-1/2 compound $ZnCu_3(OH)_6Cl_2$. Based on the analysis of the high-temperature electron spin resonance (ESR) spectra, we find its main component $|D_z| = 15(1)$ K to be perpendicular to the kagome planes. Through the temperature dependent ESR linewidth, we observe a building up of nearest-neighbor spin-spin correlations below ~150 K.

DOI: 10.1103/PhysRevLett.101.026405 PACS numbers: 71.27.+a, 75.30.Gw, 76.30.−v

Among all geometrically frustrated networks, the spin-1/2 corner-sharing kagome antiferromagnetic lattice has been at the forefront of the quest for novel quantum phenomena for the past two decades [1]. Various competing ground states with minute energy differences have been proposed [1,2] and are still under active consideration. The understanding of the ground state and of the low-lying excitations therefore still appears as a pending theoretical issue, even for the simplest nearest-neighbor (NN) isotropic Heisenberg case. In addition, minor deviations from this model, often met in experimental realizations, such as magnetic anisotropy [3,4] and spinless defects [5], may crucially affect the fundamental properties of the kagome antiferromagnets.

In the pursuit of finding a suitable compound which would reflect intrinsic kagome properties, the mineral herbertsmithite, $ZnCu_3(OH)_6Cl_2$, has recently been highlighted [6] as the first "structurally perfect" realization of the spin-1/2 kagome lattice [inset to Fig. 1(b)]. It features Cu^{2+}-based kagome planes, separated by nonmagnetic Zn^{2+}. It lacks any long-range magnetic order (LRO) down to at least 50 mK [7] despite sizable NN exchange $J \approx 190$ K [8,9]. Its bulk magnetic susceptibility χ_b monotonically increases with decreasing T [8,10], at variance with numerical calculations [9,11,12]. It was argued that this increase is due to magnetic anisotropy of the Dzyaloshinsky-Moriya (DM) type [12], $\mathbf{D}_{ij} \cdot \mathbf{S}_i \times \mathbf{S}_j$, and/or due to impurities [9,10]. Various experiments indeed evidenced 4–7% of Cu^{2+}/Zn^{2+} intersite disorder in the samples available at present [9,10,13,14]. This explains why χ_b differs significantly from the local susceptibility of the kagome planes χ_k measured by NMR [13,16]. The latter exhibits a pronounced decrease below $\sim J/2$ and shows a finite plateau at low T [13]. Together with ungapped excitations [13,15,16], this points to the absence of the singlet-triplet gap in this compound.

The absence of the spin gap leads to the important question whether this is an intrinsic feature of the kagome physics or is it related to additional terms in the Hamiltonian of $ZnCu_3(OH)_6Cl_2$. The presence and role of the DM interaction, highlighted by Rigol and Singh [12], have been questioned on several occasions [9,13,16]. Such perturbation to the isotropic Hamiltonian can indeed drastically affect the low-T properties by mixing different states and can even stabilize LRO, as in jarosites [3,17]. In order to be able to inspect this crucial issue, it is of utmost importance to experimentally determine its magnitude in $ZnCu_3(OH)_6Cl_2$.

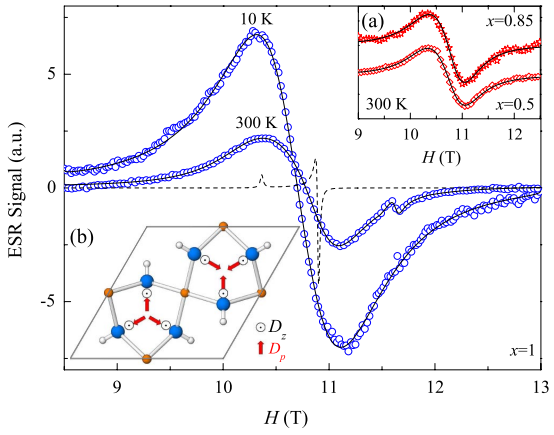

FIG. 1 (color online). ESR spectra of $Zn_xCu_{4-x}(OH)_6Cl_2$ [main panel and inset (a)], measured at 326.4 GHz, and their fits to the powder-averaged Lorentzian (solid lines). The dashed line gives an axial powder spectrum for the same g-factor anisotropy ($g_\parallel = 2.25$, $g_\perp = 2.14$) in the case of small magnetic-anisotropy broadening. Inset (b): DM vectors connecting the NN Cu^{2+} cites (middle-sized spheres) through OH^- groups (big and small spheres), with D_z and D_p as the out-of-plane and the in-plane components.

Using electron spin resonance (ESR), in this Letter we provide evidence of a sizable magnetic anisotropy, which we argue to be the DM interaction. In addition, through the temperature dependence of the linewidth, we show that spin correlations build up below $\sim$150 K and relate the low-T behavior to intersite mixing defects.

Determined by the imaginary part of the dynamical susceptibility $\chi''(\omega)$, ESR spectra, $I(\omega) \propto \chi''(\mathbf{q} \rightarrow 0, \omega) \propto \int_{-\infty}^{\infty} dt \langle S^+(t) S^-(0) \rangle \exp^{i\omega t}/T$, reflect the T-evolution of the spin correlation function $\langle S^+(t) S^-(0) \rangle$ in the direction perpendicular to the applied magnetic field H. Kramers-Krönig relations demonstrate that the integrated ESR intensity χ_{ESR} gives a locally measured static susceptibility. Further, a finite ESR linewidth provides a direct measure of a finite magnetic anisotropy.

In Fig. 1, we show typical derivative ESR spectra of polycrystalline $Zn_xCu_{4-x}(OH)_6Cl_2$ ($x = 0.5 - 1$) synthesized as in Ref. [6], which were recorded at 326.4 GHz. Using a reference sample, in $ZnCu_3(OH)_6Cl_2$ we find $\chi_{\mathrm{ESR}} = 1.0(2)$ emu/molCu at room temperature (RT), which is in good agreement with the bulk susceptibility $\chi_b = 1.1$ emu/molCu. This proves that the Cu^{2+} spins on the kagome lattice are detected by ESR [18]. The T-dependence of χ_{ESR} is presented in Fig. 2(a). Its monotonic increase with decreasing T closely resembles χ_b down to 5 K and differs from the peaked kagome planes susceptibility χ_k [13,16]. This demonstrates that ESR detects both the Cu^{2+} spins on the kagome lattice and those on the interlayer Zn sites, the latter resulting from the Zn^{2+}/Cu^{2+} intersite disorder. Despite the two detected Cu^{2+} sites with likely different g-factors ($\delta g \lesssim 0.2$), only a single ESR line is detected. This is expected [19] because the exchange coupling $J' \sim 10$ K between the two Cu^{2+} species [20] is larger than their difference in Zeeman energy, $\delta g \mu_B H \lesssim 1$ K.

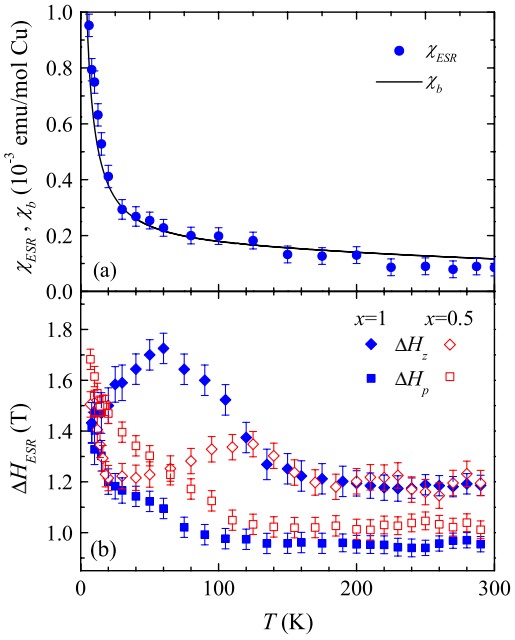

FIG. 2 (color online). (a) Scaling of ESR intensity χ_{ESR} and bulk susceptibility χ_b in $Zn_xCu_{4-x}(OH)_6Cl_2$ ($x = 1$). (b) The out-of-plane ΔH_z and the in-plane ΔH_p ESR line width.

In order to fit the spectra appropriately, one has to consider both the g-factor anisotropy and the line width broadening by the magnetic anisotropy. The former is given by $g(\theta) = [g_{\parallel}^2 \cos^2(\theta - \theta_g) + g_{\perp}^2 \sin^2(\theta - \theta_g)]^{1/2}$, where θ is the angle between H and the normal c to kagome planes. $\theta_g = 36°$ denotes the tilt of CuO_4 plaquettes with respect to the kagome planes [6], which locally sets the principal axes of the g-tensor. Typical g-factor values for Cu^{2+} ions in a uniaxial crystal field $g_{\parallel} = 2.2 - 2.4$ and $g_{\perp} = 2.05 - 2.15$ should yield two distinctive narrow features in a single ESR derivative spectrum (Fig. 1). In contrast, the observed spectra appear as a single broad derivative shape, which is a direct evidence of a sizable magnetic anisotropy. In the case of the DM interaction, which we argue below to be dominant, the symmetry of the lattice imposes the line width to depend only on θ. To fit the spectra, we therefore convoluted a powder field distribution and a Lorentzian, the latter having the semiphenomenological line width $\Delta H = (\Delta H_z^2 \cos^2\theta + \Delta H_p^2 \sin^2\theta)^{1/2}$, where ΔH_z and ΔH_p correspond to the direction parallel and perpendicular to c. The field distribution combines a uniform angular distribution and the g-factor anisotropy $g(\theta)$. Standard g-tensor values, $g_{\parallel} = 2.25$ and $g_{\perp} = 2.14$, were found. We stress that the RT ESR spectra are not noticeably affected by the Cu^{2+} spins residing on the Zn sites. They can be fitted with the same set of parameters for $x = 0.5 - 1$ (Fig. 1). We therefore use them later to determine the magnetic anisotropy in the kagome planes.

Several distinct regimes are observed in the T-dependence of the ESR line width [Fig. 2(b)]. It is constant above $\sim$200 K, with very similar values in $ZnCu_3(OH)_6Cl_2$ and $Zn_{0.5}Cu_{3.5}(OH)_6Cl_2$. This T-independence is characteristic of the high-T exchange narrowing regime. Below $\sim$150 K, a pronounced increase is observed in ΔH_z, while ΔH_p starts increasing noticeably below $\sim$100 K. On general grounds [21], we recognize the increase of the line width as the evidence of a building up of short-range spin correlations at $T \lesssim J$. The difference between ΔH_z and ΔH_p indicates that the correlations are evolving in an anisotropic manner. We propose that this results from magnetic anisotropy affecting the evolution of the correlations. With decreasing temperature, the ESR spectra should broaden monotonically as the spin correlations develop, e.g., similarly as found in another two dimensional (2D) frustrated system, $SrCu_2(BO_3)_2$ [22]. At variance, a maximum is observed in ΔH_z. Its position shifts significantly toward higher temperatures with reducing the Zn content [Fig. 2(b)]. We therefore relate this maximum to the Zn^{2+}/Cu^{2+} intersite disorder. The effect of different Cu^{2+} spins on the ESR signal is proportional to their susceptibility [19]. Therefore, below $\sim$20 K where χ_b overshadows χ_k, the Cu^{2+} spins on the Zn sites dominate the ESR response, which explains the crossover be-

tween 20 and 150 K. Weakly coupled Cu^{2+} spins on the Zn sites, with a different environment, hence a different magnetic anisotropy, would provide a natural explanation of the low-T behavior. Substantial theoretical modeling is needed though to account quantitatively for the observed line width T-dependence, which is beyond the scope of this Letter.

We address the origin and magnitude of the magnetic anisotropy in $ZnCu_3(OH)_6Cl_2$ from the detailed analysis of its RT spectrum, in the framework of the Hamiltonian

$$\mathcal{H} = J\sum_{(ij)} \mathbf{S}_i \cdot \mathbf{S}_j - g\mu_B H \sum_i S_i^z + \mathcal{H}', \qquad (1)$$

where the first sum runs oven the NN spin pairs and represents the exchange interaction $\mathcal{H}_e$, the second one gives Zeeman coupling $\mathcal{H}_Z$, and $\mathcal{H}'$ is magnetic anisotropy. For strong exchange with respect to $\mathcal{H}_Z$ and $\mathcal{H}'$, the Kubo-Tomita (KT) formalism [23] yields a Lorentzian ESR spectrum, in agreement with our experiment. Regardless of the specific form of the anisotropy, its line width can be estimated from the magnitude A of the anisotropy as $\Delta H \sim A^2/J$ [24], yielding $A \sim 16$ K.

We stress again that the spectra are extremely broad. Both the dipolar interaction between Cu^{2+} spins and their hyperfine coupling to nuclear spins are too small to account for the observed line width. They would lead to $\Delta H \lesssim 1$ mT due to strong exchange narrowing. Therefore, exchange anisotropy must be at work in $ZnCu_3(OH)_6Cl_2$. It originates from a sizable spin-orbit coupling λ, which mixes orbital excited states of Cu^{2+} with their Kramer's ground doublet, and is reflected in measured g-factor shifts of 0.14-0.25 from the free electron value 2.0023. The second-order perturbation calculation yields two exchange anisotropy terms—antisymmetric DM interaction $D \propto (\Delta g/g)J$ (linear in λ) and symmetric anisotropic exchange (AE) $\Gamma \propto (\Delta g/g)^2 J$ (quadratic in λ) [25]. The DM interaction $\mathcal{H}' = \sum_{(ij)} \mathbf{D}_{ij} \cdot \mathbf{S}_i \times \mathbf{S}_j$ is thus usually dominant in Cu-based antiferromagnets, if allowed by symmetry [25].

The out-of-plane DM component D_z is generally present in the kagome lattice, while the in-plane component D_p is allowed in $ZnCu_3(OH)_6Cl_2$ because the superexchange mediating O^{2-} ions break the mirror symmetry of the kagome planes. We therefore base our ESR analysis on the dominance of the DM anisotropy. The $\mathbf{D}_{ij}$ pattern (Fig. 1) is obtained by choosing the direction of one of the vectors and applying symmetry operators of the lattice space group. We use the convention of spins being counted clockwise in all triangles.

We can calculate the ESR line width [26]

$$\Delta H(\theta) = \sqrt{2\pi}\frac{k_b}{2g(\theta)\mu_B J} \times \sqrt{\frac{[2D_z^2 + 3D_p^2 + (2D_z^2 - D_p^2)\cos^2\theta]^3}{16D_z^2 + 78D_p^2 + (16D_z^2 - 26D_p^2)\cos^2\theta}}, \qquad (2)$$

determined by the DM pattern (Fig. 1), in the infinite-T limit. The high-T exchange narrowing regime is reached at RT since the ESR spectra do not change noticeably above ~200 K. This is consistent with a T-independent NMR spin-lattice relaxation above 150 K [16]. We fitted the RT ESR spectrum with the powder-averaged Lorentzian having the above line width $\Delta H(\theta)$. In Fig. 3, we plot on the $D_z - D_p$ map the reduced χ^2 obtained from the fit. Optimal parameters are $|D_z| = 15(1)$ K and $|D_p| = 2(5)$ K. According to Eq. (2), their sign cannot be determined by ESR. We find the magnitude of the extracted DM interaction ($D/J \approx 0.08$) in the range set by several other Cu-based 2D frustrated systems. For instance, in the orthogonal-dimer system $SrCu_2(BO_3)_2$, it amounts to 4% of the isotropic exchange [22,27], while the ratio of 16% was reported for the triangular compound Cs_2CuCl_4 [28].

At this point, it is important to address the issue of the possible hidden symmetry of the DM interaction [29]. For linear spin chains with staggered DM vectors, one can effectively transform it to the AE term of the magnitude D^2/J by applying a nonuniform spin rotation [30]. This makes it of the same order as the initial AE and discards the direct applicability of the KT formalism [30,31]. However, for other lattices, one should distinguish between reducible DM components, transforming to λ^2 order, and irreducible components, remaining linear in λ [27]. The components that can be eliminated in the first order are those which sum up to zero within any closed loop on the lattice [27]. For the kagome lattice, the in-plane D_p is reducible while the out-of-plane D_z is irreducible. Using the KT formalism for the latter is therefore well justified, while the former might not be accurate. However, the small value of D_p does not significantly influence the ESR spectra (see Fig. 3). We note that in $SrCu_2(BO_3)_2$, the values of the DM interaction obtained from the KT analysis [22], from inelastic neutron scattering [27], and from NMR measurements [32] were found to agree within 20%.

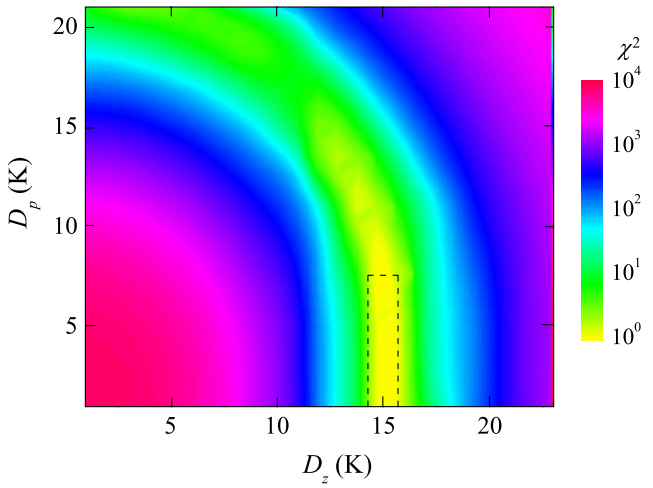

FIG. 3 (color online). The reduced χ^2, reflecting the quality of the RT fit in $ZnCu_3(OH)_6Cl_2$. The dashed rectangle gives the optimal parameters $|D_z| = 15(1)$ K and $|D_p| = 2(5)$ K.

In Ref. [12], somewhat larger values, $|D_z| \approx 0.1J$ and $|D_p| \approx 0.2 - 0.3J$, than extracted in this study were suggested to explain the bulk susceptibility upturn in $ZnCu_3(OH)_6Cl_2$, by considering the DM interaction as the only additional term to the Heisenberg Hamiltonian. These values would lead to high-T ESR line widths of 6–7 T, which is inconsistent with our experimental observations. Therefore, DM interaction alone cannot account for the macroscopic susceptibility in $ZnCu_3(OH)_6Cl_2$.

Sizable DM interaction ($D/J \approx 0.08$) raises the fundamental question to what extent DM anisotropy affects the low-T magnetism of $ZnCu_3(OH)_6Cl_2$. Spin-wave excitations in the spin-5/2 Fe-jarosite were explained by the presence of the DM interaction of a similar magnitude ($D/J \approx 0.09$) [17]. In this kagome compound, Néel order below 65 K was reproduced by classical Monte Carlo calculations, predicting uniform ($\mathbf{q} = 0$) ordered spin structures induced by the DM interaction [3]. In the $S = 1/2$ case, quantum correction should suppress LRO for small D/J [4]. For $D/J \gtrsim 0.05$, recent numerical calculations seem to indicate a broken-symmetry state at $T = 0$, which however has no on-site magnetic moment [33]. Further, the rather large Cu^{2+}/Zn^{2+} intersite disorder may destabilize LRO. Indeed, vacancies on the spin-1/2 Heisenberg kagome lattice induce unexpectedly extended dimer-dimer correlations, despite short-ranged spin-spin correlations [5]. Although exact dimer patterns are not known for additional terms in the Hamiltonian that break the SU(2) symmetry, it seems plausible that they would contradict the uniform LRO state preferred by the DM interaction. This might explain the absence of LRO in $ZnCu_3(OH)_6Cl_2$ down to $D/300 = 50$ mK.

Last, quite importantly, the DM interaction mixes magnetic excitations into the presumably singlet ground state of the Heisenberg kagome lattice. This could explain the experimentally observed gapless excitation spectrum in $ZnCu_3(OH)_6Cl_2$ [13,16] and the finite susceptibility of kagome planes at low T [13], as confirmed by numerical calculations on finite spin clusters [34]. These experimental results could likewise be described as a disorder-generated effect, due to a vacancy-induced spatially distributed density of states [35]. Most likely, both effects play an important role.

In conclusion, we have shown that the DM interaction in $ZnCu_3(OH)_6Cl_2$ is sizable ($D/J \approx 0.08$) and could critically affect the low-T properties. Knowing its magnitude, future theoretical studies should investigate its impact on the ground state. They should also clarify whether the DM magnetic anisotropy and the Cu^{2+}/Zn^{2+} intersite disorder are primarily responsible for the absence of the spin gap.

We acknowledge discussions with B. Canals, O. Cépas, C. Lacroix, C. Lhuillier, G. Misguich, and S. El Shawish. The work was supported by the EC MC Grant No. MEIF-CT-2006-041243, the ANR Project No. NT05-4_41913, and the ARRS Project No. Z1-9530. NHMFL is supported by NSF (No. DMR-0654118) and the State of Florida.

[1] For a review, see G. Misguich and C. Lhuillier, *Frustrated Spin Systems*, edited by H. T. Diep (World-Scientific, Singapore, 2005).
[2] Y. Ran *et al.*, Phys. Rev. Lett. **98**, 117205 (2007); S. Ryu *et al.*, Phys. Rev. B **75**, 184406 (2007); R. R. P. Singh and D. A. Huse, Phys. Rev. B **76**, 180407(R) (2007).
[3] M. Elhajal *et al.*, Phys. Rev. B **66**, 014422 (2002).
[4] R. Ballou *et al.*, J. Magn. Magn. Mater. **262**, 465 (2003).
[5] S. Dommange *et al.*, Phys. Rev. B **68**, 224416 (2003).
[6] M. P. Shores *et al.*, J. Am. Chem. Soc. **127**, 13462 (2005).
[7] P. Mendels *et al.*, Phys. Rev. Lett. **98**, 077204 (2007).
[8] J. S. Helton *et al.*, Phys. Rev. Lett. **98**, 107204 (2007).
[9] G. Misguich and P. Sindzingre, Eur. Phys. J. B **59**, 305 (2007).
[10] F. Bert *et al.*, Phys. Rev. B **76**, 132411 (2007).
[11] N. Elstner and A. P. Young, Phys. Rev. B **50**, 6871 (1994).
[12] M. Rigol and R. R. P. Singh, Phys. Rev. Lett. **98**, 207204 (2007); Phys. Rev. B **76**, 184403 (2007).
[13] A. Olariu *et al.*, Phys. Rev. Lett. **100**, 087202 (2008).
[14] M. A. de Vries *et al.*, Phys. Rev. Lett. **100**, 157205 (2008).
[15] O. Ofer *et al.*, arXiv:cond-mat/0610540.
[16] T. Imai *et al.*, Phys. Rev. Lett. **100**, 077203 (2008).
[17] K. Matan *et al.*, Phys. Rev. Lett. **96**, 247201 (2006).
[18] The intensity of the small impurity-phase signal observed around 11.6 T is ca. 0.2% of the total ESR intensity.
[19] J. E. Gulley and V. Jaccarino, Phys. Rev. B **6**, 58 (1972).
[20] This order of magnitude is inferred from the magnetic ordering temperature (6–19 K) of the $Zn_xCu_4 - x(OH)_6Cl_2$ compounds with $x < 1$ [6,7].
[21] P. M. Richards, *Local Properties of Low-Dimensional Antiferromagnets*, edited by K. A. Müller (Nord Holland Publishing Company, Amsterdam, 1976).
[22] A. Zorko *et al.*, Phys. Rev. B **69**, 174420 (2004).
[23] R. Kubo and K. Tomita, J. Phys. Soc. Jpn. **9**, 888 (1954).
[24] T. G. Castner, Jr. and M. S. Seehra, Phys. Rev. B **4**, 38 (1971).
[25] T. Moriya, Phys. Rev. **120**, 91 (1960).
[26] The ESR line width $\Delta H = \sqrt{2\pi} k_B/(g\mu_B)\sqrt{M_2^3/M_4}$ is for $k_BT \gg g\mu_BH$ given by the second and the fourth moment, $M_2 = \langle[\mathcal{H}', S^+][S^-, \mathcal{H}']\rangle/\langle S^+S^-\rangle$ and $M_4 = \langle\{\mathcal{H} - \mathcal{H}_Z, [\mathcal{H}', S^+]\}\{\mathcal{H} - \mathcal{H}_Z, [\mathcal{H}', S^-]\}\rangle/\langle S^+S^-\rangle$ [24].
[27] Y. F. Cheng *et al.*, Phys. Rev. B **75**, 144422 (2007).
[28] R. Coldea *et al.*, Phys. Rev. Lett. **88**, 137203 (2002).
[29] T. A. Kaplan, Z. Phys. B **49**, 313 (1983); L. Shekhtman, O. Entin-Wohlman, and A. Aharony, Phys. Rev. Lett. **69**, 836 (1992).
[30] J. Choukroun *et al.*, Phys. Rev. Lett. **87**, 127207 (2001).
[31] M. Oshikawa and I. Affleck, Phys. Rev. B **65**, 134410 (2002).
[32] K. Kodama *et al.*, J. Phys. Condens. Matter **17**, L61 (2005).
[33] O. Cépas *et al.*, arXiv:cond-mat/0806.0393 (to be published).
[34] S. El Shawish (private communications).
[35] K. Gregor and O. I. Motrunich, Phys. Rev. B **77**, 184423 (2008).